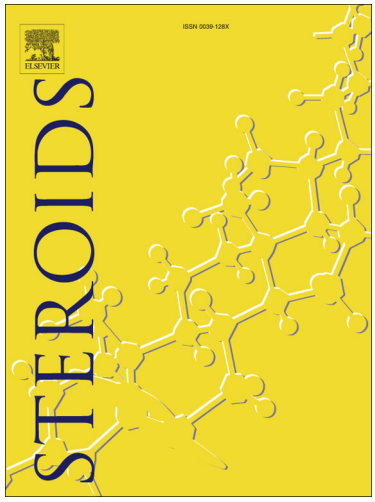

Identification of D-seco modified steroid derivatives with affinity for estrogen receptor α and β isoforms using a non-transcriptional fluorescent cell assay in yeast

Sofija S. Bekić, Maja A. Marinović, Edward T. Petri, Marija N. Sakač, Andrea R. Nikolić, Vesna V. Kojić, Andjelka S. Ćelić

PII: S0039-128X(17)30228-3
DOI: https://doi.org/10.1016/j.steroids.2017.12.002
Reference: STE 8199

To appear in: *Steroids*

Received Date: 15 June 2017
Revised Date: 1 December 2017
Accepted Date: 4 December 2017

Please cite this article as: Bekić, S.S., Marinović, M.A., Petri, E.T., Sakač, M.N., Nikolić, A.R., Kojić, V.V., Ćelić, A.S., Identification of D-seco modified steroid derivatives with affinity for estrogen receptor α and β isoforms using a non-transcriptional fluorescent cell assay in yeast, *Steroids* (2017), doi: https://doi.org/10.1016/j.steroids.2017.12.002

Identification of D-seco modified steroid derivatives with affinity for estrogen receptor α and β isoforms using a non-transcriptional fluorescent cell assay in yeast

Sofija S. Bekić[a], Maja, A. Marinović[b], Edward T. Petri[b], Marija N. Sakač[a], Andrea R. Nikolić[a], Vesna V. Kojić[c], Andjelka S. Ćelić[b,*]

[a]*University of Novi Sad, Faculty of Sciences, Department of Chemistry, Biochemistry and Environmental Protection, Trg Dositeja Obradovića 3, 21000 Novi Sad, Serbia*

[b]*University of Novi Sad, Faculty of Sciences, Department of Biology and Ecology, Trg Dositeja Obradovića 2, 21000 Novi Sad, Serbia*

[c]*University of Novi Sad, Faculty of Medicine, Oncology Institute of Vojvodina, Put doktora Goldmana 4, 21204 Sremska Kamenica, Serbia*

*Corresponding author:
Dr. Andjelka S. Ćelić
University of Novi Sad
Faculty of Sciences
Department of Biology and Ecology
Trg Dositeja Obradovića 2, 21000 Novi Sad, Serbia
E-mail: andjelka.celic@dbe.uns.ac.rs
Tel: +381 21 485 2715

Abstract

Synthesis and biological evaluation of steroidal derivatives with anticancer properties is an active area of drug discovery. Here we measured the relative affinities of D-seco modified steroidal derivatives for estrogen receptor α, estrogen receptor β or androgen receptor ligand binding domains using an optimized non-transcriptional fluorescent cell assay in yeast. Ligand binding domains of steroid receptors were expressed in-frame with yellow fluorescent protein in the yeast *Sacharomyces cerevisiae.* Addition of known steroid ligands to yeast expressing the appropriate cognate receptor results in increased fluorescence intensity, enabling estimation of receptor binding affinities in a dose-response and time-dependent manner. Relative binding affinities of D-seco modified steroidal derivatives **1**-**4** were then evaluated using this yeast system by live cell fluorimetry and fluorescence microscopy, coupled with *in vitro* cytotoxicity and *in silico* molecular docking studies. D-seco estratriene derivative **2**displayed strong affinity for both estrogen receptor α and β ligand binding domains and negligible affinity for the androgen receptor ligand binding domain**.** Compound **2** also showed moderate cytotoxicity against estrogen receptor positive MCF-7 breast adenocarcinoma cells. In addition to identification of new ligands for steroid receptors, this assay could also be used to filter out compounds with potential for off-target interactions with steroid receptors during the early stages of compound screening.

Keywords

estrogen receptor, steroid derivative, biosensor, yellow fluorescent protein, breast cancer, molecular docking

1. Introduction

Hormone-sensitive breast and prostate cancers are leading causes of death worldwide, and modulation of steroid signaling is an effective treatment strategy [1]. Hormonal steroids and their metabolites influence the proliferation of hormone-responsive (*e.g.* ovarian, prostate, endometrial and breast) and other cancers (*e.g.* cervical and colorectal) [2]. The ability to selectively interfere with steroid hormone signaling in these cancers may lead to improved strategies for prevention and treatment.

Steroid hormones carry out their physiological effects by binding steroid receptors that function as ligand-activated transcription factors. Steroid receptors consist of two functional units: DNA-binding and ligand-binding domains (LBD). Steroid receptor activation involves dimerization of the receptor after ligand binding, translocation of the complex to the nucleus and interaction with co-regulatory proteins and specific DNA sequences, resulting in transcription of target genes [3]. Estrogen receptor (ER) signaling plays a major role in the development and growth of normal breast epithelium, as well as malignant transformations [4]. Two ER isoforms, ERα and ERβ, have been identified with sequence and structural homology but differences in tissue distribution [5]. Both ER isoforms are involved in breast cancer progression, while a relationship may exist between ERβ and colon adenocarcinoma [6]. Similarly, androgen receptor (AR) is associated with prostate development as well as prostate cancer progression [7].

Several steroidal anticancer drugs in use against breast or prostate cancer (*e.g.* exemestane, abiraterone) inhibit steroidogenic enzymes; while others (*e.g.* fulvestrant, megestrol and cyproterone) target hormone receptors. For example, fulvestrant blocks breast cancer proliferation by binding and destabilizing ERα and has been effective in the treatment of hormone-sensitive advanced breast cancer [8]. In contrast, activation of steroid hormone

signaling by agonists may be effective for conditions such as osteoporosis [9] and menopause [10]. Because of the prevalance of cancers resistant to current treatments, characterization of steroidal derivatives with anticancer properties remains necessary.

Our group previously synthesized D-seco steroidal derivatives (**1-4**) (**Figure 1**), with antiproliferative (**1**) and antiestrogenic (**2-4**) properties suggesting interaction with ER signaling. Steroidal 16,17-seco-16,17a-dinitrile (**1**) displayed selective submicromolar antiproliferative activity against hormone dependent and independent breast cancer cells; while a 17-bromo derivative of 16,17-seco-estratriene-16-nitrile (**2**) and other 16,17-substituted-16,17-seco-estratrienes (**3-4**) exhibited antiestrogenic activity in a uterotrophic assay [11–15]. We hypothesize that D-seco derivatives of steroid receptor ligands may retain affinity for their steroid receptor while perturbing intermolecular interactions necessary for receptor activation [16].

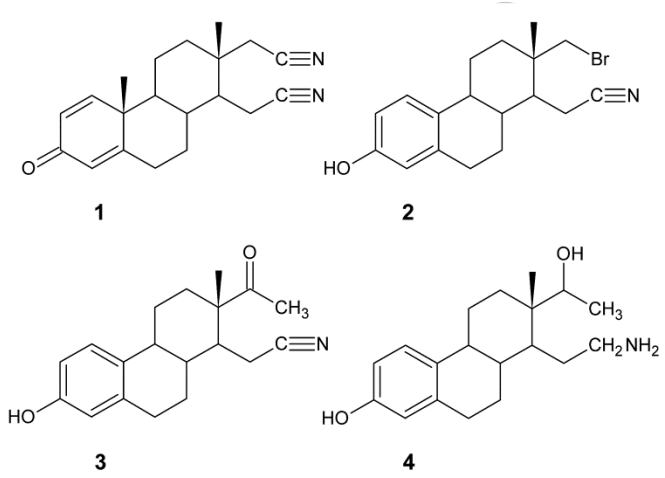

Figure 1. Chemical structures of tested D-seco steroid derivatives: **1** (3-Oxo-16,17-secoandrosta-1,4-diene-16,17a-dinitrile), **2** (3-Hydroxy-17-bromo-16,17-secoestra-1,3,5(10)-triene-16-nitrile), **3** (3-Hydroxy-17-methyl-17-oxo-16,17-secoestra-1,3,5(10)-triene-16-nitrile) and **4** (16-Amino-17-methyl-16,17-secoestra-1,3,5(10)-triene-3,17-diol)

Therefore, in the present study we set out to evaluate the relative binding affinities of **1-4** for ERα, ERβ and AR. Although sensitive transcription-based activation assays for ERα and AR have been reported using mammalian cell cultures, test compounds can be metabolized. In contrast, yeast have low metabolic activities, meaning screening results should correspond to the bioactivity of the original synthetic product. In addition, yeast do not express endogenous steroid receptors, reducing cross-activation by other signaling pathways. Furthermore, yeast cells are highly robust and tolerate many of the solvents and byproducts present following organic synthesis of steroids [17,18]. Transcription-based assays, such as the yeast estrogen screen (YES) or yeast androgen screen (YAS) involve ligand-mediated activation of ERα or AR, translocation to the nucleus and activation of the expression of a reporter gene such as β-galactosidase or green fluorescent protein (GFP) [17,19]. Expression of GFP is monitored by fluorescence while measurement of β-galactosidase induction requires additional chemicals and cell lysis for detection. Possible disadvantages include reports that partial ERα antagonists such as tamoxifen activate ERα in transcription-based assays, leading to potential ambiguity in identification of new antagonists or agonists [19]. Also, reporter gene based assays require completion of steps beyond ligand binding, including nuclear translocation, binding to DNA and activation of cell transcription machinery. Such transcription-based screens might miss compounds that bind steroid receptors but are inefficient at inducing all of the steps necessary for reporter gene activation [18].

Because of the above, in the present study we optimized a non-transcriptional assay originally reported by Muddana and Peterson [20] (**Figure 2**). In this assay, LBDs of ERα, ERβ and AR are expressed in-frame with yellow fluorescent protein (YFP) in yeast: enabling fluorescent resonance energy transfer (FRET) between two YFP molecules upon receptor

dimerization [21]. Because receptor dimerization is ligand-dependent, fluorescence intensity correlates with ligand binding affinity [20]. Relative binding affinities of D-seco derivatives **1**-**4** were evaluated using two methods: live cell fluorimetry and fluorescence microscopy. Compounds were also tested for *in vitro* cytotoxicity against two human tumor cell lines, ER+ breast adenocarcinoma (MCF-7) and prostate cancer (PC3), and one human non-cancerous cell line, normal fetal lung fibroblasts (MRC-5), as well as *in silico* molecular docking studies against X-ray crystal structures of ERα and ERβ.

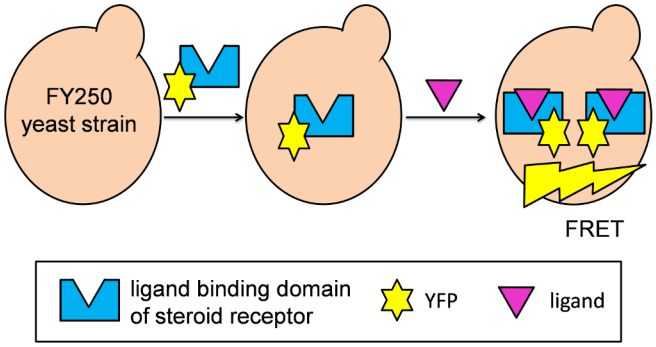

Figure 2. Schematic of the fluorescent cellular biosensor. Expression of the LBDs of selected steroid receptors fused with YFP in *Sacharomyces cerevisiae* FY250 strain. Ligand binding induces steroid receptor dimerization causing increased fluorescence due to FRET between two YFP molecules. The intensity of fluorescence correlates with ligand binding affinity.

2. Materials and methods

2.1. Chemicals

Yeast nitrogen base without amino acids, yeast synthetic drop-out medium supplements without tryptophan, raffinose, galactose, steroid hormones and tamoxifen were purchased from Sigma-Aldrich. Solvent dimethyl-sulfoxide (DMSO) was purchased from Lach-Ner. Test compounds **1**-**4** were synthesized in our laboratory as previously described: **1** (3-Oxo-16,17-secoandrosta-1,4-diene-16,17a-dinitrile) [11], **2** (3-Hydroxy-17-bromo-16,17-secoestra-1,3,5(10)-triene-16-nitrile) [12,13], **3** (3-Hydroxy-17-methyl-17-oxo-16,17-secoestra-1,3,5(10)-

triene-16-nitrile) and **4** (16-Amino-17-methyl-16,17-secoestra-1,3,5(10)-triene-3,17-diol) [14]. Stock solutions of all test compounds were freshly prepared in DMSO. All reagents were of analytical grade and used without further purification.

2.2. Yeast strains, plasmids and growth conditions

Saccharomyces cerevisiae FY250 strain (MATα, *ura3-52, his32Δ00, leu2Δ1, trp1Δ6)* and plasmid constructs pRF4-6-hERα LBD-EYFP, pRF4-6-hERβ LBD-EYFP and pRF4-6-hAR LBD-EYFP (in further text LBD-YFP) for the fluorescent cellular sensor used in this study, were generously provided by Dr. Blake Peterson (The University of Kansas) [20]. Expression of all LBD-YFP proteins is under control of galactose-inducible GAL1 promoter. We used a standard lithium acetate/polyethylene glycol method for yeast transformation with these LBD-YFP expression vectors [22]. Selection of transformants was performed on tryptophan dropout plates for 3 days at 30^{o}C. Selected individual transformed colonies were picked and restreaked onto a master plate.

2.3. Fluorescent cellular assay

Pre-cultures were grown to saturation at 28^{o}C in selection media (yeast nitrogen base without amino acids and appropriate dropout powder) supplemented with 2% raffinose with agitation and aeration. Recombinant strains were initially grown in raffinose instead of glucose as a carbon source, because raffinose relieves glucose repression of the GAL1 promoter without inducing expression [23]. Expression of LBD-YFP proteins can then be induced by adding galactose to the growth media [23]. Cell density was determined by measuring absorbance at 600 nm (optical density, OD_{600}) on a spectrophotometer plate reader (ThermoLabsystems Multiscan EX). Saturated yeast cells were diluted in fresh selection media supplemented with 2% raffinose at an OD_{600} of 0.1. Fresh culture was incubated under identical conditions until cells reached

logarithmic phase of growth, OD_{600} of 0.4-0.6 and 2-3 doublings occurred (approximately 12h). In mid logarithmic phase of growth, expression of LBD-YFP proteins was induced by addition of galactose to the growth media to a final concentration of 2%. Simultaneously, test compounds **1**-**4** were added to final concentrations of 10 μM. High-affinity ER ligands, tamoxifen [24] and estrone and a low-affinity ligand androstenedione, were used as positive and negative controls, respectively, in cells expressing LBD of ERα and ERβ. For cells expressing the LBD of AR, androstenedione was used as a positive control, high affinity ligand, whereas tamoxifen and estrone were used as negative controls. All ligands were used at the same final concentration of 10 μM. In order to test for solvent fluorescence, DMSO without ligand was added to a final concentration of 1% (DMSO control). Additionally, an aliquot of cell culture without added galactose and ligand served as an uninduced control. Incubation was continued at 25°C for 14-16 h in the dark. At or below room temperature more efficient expression and folding of green fluorescent protein variants, such as YFP, has been reported [25]. Finally, fluorescence intensity following 14-16 h expression of LBD-YFP fusion proteins in the presence or absence of added ligand was measured using two different detection methods: fluorescence microscopy and fluorescence measurements in 96-well format.

2.3.1. Fluorescence microscopy

Fluorescence microscopy was used to visualize expressed YFP protein fused with the appropriate LBD in recombinant yeast cells. To obtain a large number of cells per field of view, useful for further image analysis, cells were concentrated five-fold by centrifugation for 10 min at 5000 x g. For visualization, 10 μl of each cell suspension was taken and observed under the fluorescence microscope (Axio Imager 2) using a FITC filter (excitation of 485 nm and emission of 535 nm) and 40 x objective. In order to test the method, dose-response and time-dependence

curves were created. For dose response curves, the change in mean fluorescence of yeast cells expressing AR LBD-YFP was measured by fluorescence microscopy upon addition of the known AR ligand, dihydrotestosterone, at six different concentrations (0.001, 0.01, 0.1, 1, 10 and 100 μM) and 16h exposure time. A similar dose response curve was created for yeast cells expressing ERβ LBD-YFP using estradiol as a known ligand (see supplemental data). Time-dependent changes in mean fluorescence were also monitored in yeast cells expressing ERβ LBD-YFP in the presence of the ERβ ligand, estradiol, at a final concentration of 10 μM over a period of 30 h.

2.3.2. ImageJ analysis

Images were analyzed by densitometry using ImageJ freeware [26]. Bright-field and appropriate fluorescent images were overlapped. Background signal was then subtracted. Cells were manually outlined and the mean pixel intensity of outlined regions was determined. This value is directly proportional to the mean fluorescence intensity of a cell. Fifty cells per sample were analyzed. Ligand binding affinity was expressed as fold fluorescence to DMSO control and calculated as follows:

$$fold\ fluorescence = \frac{mean\ fluorescence\ intensity\ of\ the\ cell_{sample}}{mean\ fluorescence\ intensity\ of\ the\ cell_{DMSO\ control}} \quad (1)$$

Histograms were plotted using Origin Pro 8, data analysis software. Error bars represent propagated standard errors of the mean (SE).

2.3.3. Fluorescence measurement in 96-well format

For fluorescence readings aliquots of 100 μl intact cell suspension were added to a 96-well microplate (Carl Roth). Wells containing growth medium were used as a blank. All samples were tested in triplicate. Cell density was determined by measuring the absorbance at 600 nm. Fluorescence intensity was measured at 25°C using excitation and emission wavelengths of 485 nm and 538 nm, respectively on a fluorimeter (Fluoroskan Ascent FL). The plate was shaken

each time before measurements to avoid aggregation of yeast cells. Fluorescence intensity values represent the mean of three probes. Ligand binding affinity was expressed as fold fluorescence to DMSO control and calculated as follows:

$$fold\ fluorescence = \frac{fluorescence\ intensity\ per\ cell_{sample} - fluorecence\ intensity\ per\ cell_{uninduced}}{fluorescence\ intensity\ per\ cell_{DMSO\ control} - fluorecence\ intensity\ per\ cell_{uninduced}} \quad (2)$$

Histograms were plotted using Origin Pro 8, data analysis software. Error bars represent propagated standard errors of the mean (SE).**2.4. Cell lines**

Two human tumor cell lines, ER+ breast adenocarcinoma (MCF-7) and prostate cancer (PC3), and one human non-cancerous cell line, normal fetal lung fibroblasts (MRC-5), were used in *in vitro* cytotoxicity assays. Cells were grown in Dulbecco's modified Eagle's medium (DMEM) with addition of 4.5% glucose. The medium was supplemented with 10% of fetal calf serum (FCS, Sigma) and antibiotics (100 IU/mL of penicillin and 100 μg/ml of streptomycin (Sigma). Cells were cultured in flasks (Costar, 25 cm^3) at 37°C in 100% humidity atmosphere with 5% CO_2. Only viable cells, as determined by dye exclusion assay, were used in the cytotoxicity assay.

2.5. Cytotoxicity assay

In vitro cytotoxic activity of test compounds against all cell lines was evaluated by the tetrazolium colorimetric MTT assay [27]. Cells were exposed to test compounds **2**-**4** and doxorubicin for a period of 48 h, in a concentration range from 10^{-8} to 10^{-4} M.

MTT assay is based on cleavage of the 3-(4,5-dimethylthiazol-2-yl)-2,5-diphenyl tetrazolium bromide (MTT), to formazan by mitochondrial dehydrogenases in viable cells. Exponentially growing cells were harvested, counted by trypan blue exclusion and plated onto 96-well microplates (Costar) at an optimal seeding density of 5×10^3 cells per well to assure logarithmic growth rate throughout the assay period. Viable cells were plated in a volume of 90

µl per well, and preincubated in complete medium at 37 °C for 24 h to ensure cell stabilization prior to the addition of substances. Test compounds, at 10 x the required final concentration, in growth medium (10 µl per well) were added to all wells except controls and microplates were incubated for 48 h. The wells containing cells without tested compounds were used as control. Three hours before the end of incubation period, 10 µl of MTT solution was added to each well. MTT was dissolved in medium at 5 mg/ml and filtered to sterilize and remove a small amount of insoluble residue present in some batches of MTT. Acidified 2-propanol (100 µl of 0.04 M HCl in 2-propanol) was added to each well and mixed thoroughly to dissolve the dark blue crystals. After a few minutes at room temperature to ensure that all crystals were dissolved, plates were read on a spectrophotometer plate reader (Multiscan MCC340, Labsystems) at 540/690 nm. Wells without cells, containing complete medium and MTT served as a blank. Doxorubicin was used as a nonspecific cytotoxicity control. The cytotoxicity was expressed as IC_{50} (the concentration required to inhibit the growth of the cells by 50%). The IC_{50} of each test compound was determined by Median effect analysis.

2.6. Molecular docking

2.6.1. Protein (receptor) structural coordinate preparation

Three-dimensional structural coordinates for ERα-LBD (PDB ID: 1A52 [28]) and ERβ-LBD (PDB ID: 3OLS [29]) were obtained from the Protein Data Bank [30,31]. Coordinates for ligands and all water molecules were removed using a text editor. Hydrogen atoms and Gasteiger partial charges were added using the script 'receptor.c' in VEGA ZZ 3.1.0 [32]. Nonpolar hydrogen atoms were merged in VEGA ZZ and receptor coordinates were saved in PDBQT format for docking simulations.

2.6.2. Ligand structural coordinate preparation

Structural models of compounds **1**-**4** were created using AVOGADRO 1.1.1 [33,34]. Hydrogen atoms were added and ligand geometries were optimized (MMF94s forcefield: 500 steps of conjugate gradient energy minimization followed by 500 steps of steepest descent energy minimization with a convergence setting of $10x10^{-7}$) in the program AVOGADRO. Nonpolar hydrogen atoms were merged and Gasteiger partial charges were calculated using the script 'ligand.c' in VEGA ZZ 3.1.0 and the resulting ligand coordinate files were saved in PDBQT format. cLogP values were calculated for each compound in the program VEGA.

2.6.3. Grid parameter file preparation

Grid maps were calculated for each receptor using AutoGrid 4 and AutoDockTools [35], based on ligand coordinates present in crystal structures. Individual grid maps were centered on each protein molecule and a default box size of 50x50x50 points with default grid spacing of 0.375 Å was chosen. Maps were calculated for each atom type (including hydrogen bond donors, acceptors and aromatic atoms) in the ligand along with an electrostatic and desolvation map using a default dielectric value of –0.1465.

2.6.4. Docking parameter file preparation and molecular docking simulations

Initial ligand position, orientation and dihedral offset values were set as random. The number of torsional degrees of freedom (i.e. rotatable bonds) for each ligand was determined during the ligand preparation stage in AutoDockTools [35]. Molecular docking studies were conducted using the Lamarckian genetic algorithm. The maximum number of energy evaluations was set to 2500000 and the GA population size was 150. A total of 50 hybrid GA-LS runs were performed for each simulation. Results were visualized using PyMOL [36] and compared to X-ray structures of ligand bound receptor complexes (1A52 for ERα and 3OLS for ERβ). AutoGrid and AutoDock calculations were run remotely at the National Biomedical Computational

Resource [37,38] using the PyRx virtual screening tool [39]. All control redocking simulations using ligands from X-ray crystal structures correctly reproduced ligand-protein geometries found in their respective X-ray structures. Based on these control docking simulations, predicted binding energies ≤ -10.21 kcal/mol (ERα) and ≤ -10.77 kcal/mol (ERβ) were indicative of strong binding.

3. Results and discussion

3.1. Optimization of a non-transcriptional fluorescent cell assay in yeast for detection of steroid receptor ligands

Previous observations suggest that D-seco steroid derivatives **1-4** may have antiproliferative (**1**) or antagonist properties (**2-4**) involving ER signaling [11–15]. To estimate the relative binding affinities of **1-4** for ERα, ERβ and AR, we chose to optimize a non-transcriptional fluorescent assay in yeast reported by Muddana and Peterson, that directly measures binding of ligands to the LBD of steroid receptors [20]. Using flow cytometry, this assay has a reported sensitivity similar to transcription-based yeast screens for known ERα or AR ligands. However, the sensitivity required for characterization of purified synthetic steroidal derivatives is less than that for envirionmental or biomedical samples. Thus, in the present study the assay was optimized to quickly estimate the affinities of steroidal derivatives by fluoresence microscopy or spectroscopy using standard laboratory equipment. Results from this assay can be combined with results from other tests of bioactivity to guide organic synthesis efforts. In fact, it is often a goal of organic synthesis to develop steroidal compounds with *no* detectable affinity for ERα or AR, to reduce off-target activation of ER or AR signaling: for example in the design of steroidal inhibitors of aromatase (CYP19) or 17α-hydroxylase (CYP17) for the treatment of hormone-sensitive cancers [40].

Ligand binding domains of ERα, ERβ and AR fused to YFP were expressed in yeast under control of a GAL1-inducible promoter and detected by fluoresence microscopy. Because ligand binding may stabilize folding of LBD-YFP proteins during expression [20], test ligands were added simultaneously with galactose used for induction of YFP expression, resulting in improved cell fluorescence (not shown). As can be seen in results from a typical experiment (**Figure 3**) cell fluorescence intensity rises sigmoidally with increasing ligand concentration, reaching saturation at 100 μM (**Figure 3A**). Similarly, upon addition of test ligand at 10μM, cell fluorescence intensity increases with increasing exposure time, reaching saturation after 15 h (**Figure 3B**).

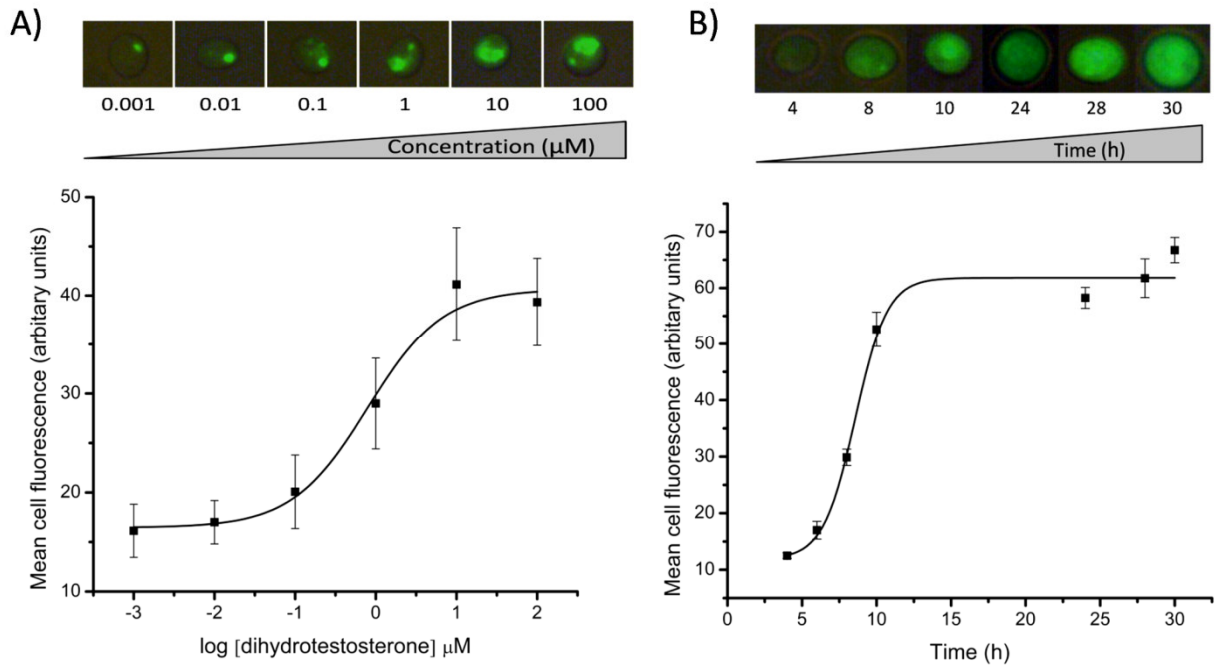

Figure 3. A) Dose-response curve. Change in mean fluorescence of yeast cells (n=15) expressing AR LBD-YFP upon addition of the AR ligand, dihydrotestosterone, at six different concentrations (0.001, 0.01, 0.1, 1, 10 and 100 μM) and 16 h exposure time. The concentration range on the X axis is given in logarithmic scale. B) Time-dependent change in mean fluorescence of yeast cells (n=8) expressing ERβ LBD-YFP in the presence of the ERβ ligand, estradiol, at a final concentration of 10 μM. In both cases mean cell fluorescence was determined by analyzing fluorescence images by densitometry using ImageJ. Data were fitted in Origin Pro 8 using sigmoidal curve fitting. Error bars represent standard errors of the mean.

3.2. Measurement of the relative binding affinities of ligands for ERα, ERβ and AR by live cell fluorescence microscopy

A panel of bright field and fluorescence micrographs of live recombinant yeast cells expressing ERα LBD-YFP, ERβ LBD-YFP or AR LBD-YFP exposed to different test ligands vs. controls is shown in **Figure 4**. In the absence of galactose (uninduced control), no fluorescence was detectable, while baseline YFP fluorescence was observed in cells upon induction of expression of each receptor LBD-YFP construct with galactose. In the absence of ligand (DMSO control), fluorescence was found to be localized for all LBD-YFP constructs and the least intense in cells expressing AR LBD-YFP.

Yeast expressing ERα LBD-YFP or ERβ LBD-YFP were treated with tamoxifen [24] or estrone as high-affinity ER ligands (positive control) and compared with the same cells treated with androstenedione, a steroidal ligand expected to have low-affinity for both ER isoforms (negative control). For yeast cells expressing the AR LBD-YFP, androstenedione was considered to be a high-affinity AR ligand (positive control), while tamoxifen or estrone were low-affinity AR ligands (negative control). As can be seen in **Figure 4**, addition of high-affinity ligands to cells expressing the corresponding cognate receptor resulted in a strong increase in fluorescence intensity, coupled with a visual change in the cellular distribution of YFP. In agreement with previous observations, ligand binding appears to induce a redistribution of steroid receptor LBD-YFP fusions from some intracellular organelle (presumably the endoplasmic reticulum) to the cytoplasm [20]. This change in cellular localization provides a rapid qualitative measure of the potential bioactivity of test compounds using fluoresence microscopy.

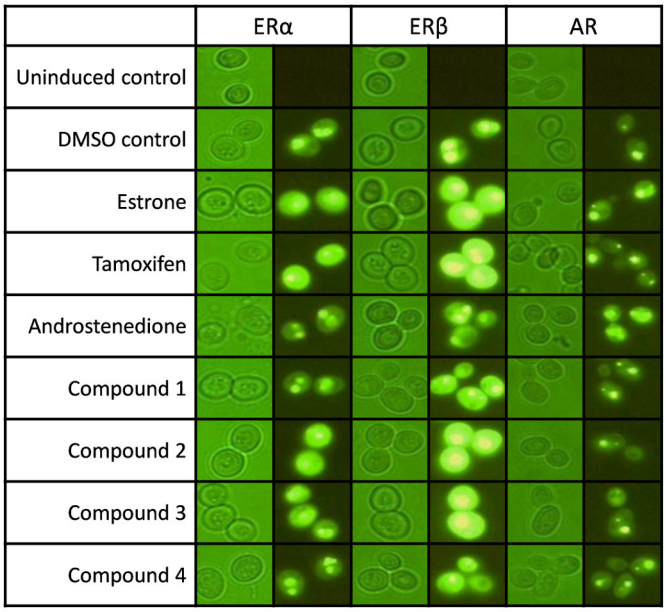

Figure 4. Representative bright field and fluorescence micrographs of recombinant yeast cells expressing ERα LBD-YFP, ERβ LBD-YFP and AR LBD-YFP tretated with DMSO (DMSO control), estrone, tamoxifen, androstenedione, or test compounds **1**-**4** at a final concentration of 10 μM for 14-16h vs. uninduced cells (uninduced control). All fluorescence micrographs were captured with an identical exposure time of 500 ms using a FITC filter. Cell fluorescence intensity correlates with relative ligand binding affinity for these receptors.

To quantitate the affinities of **1-4** for ERα, ERβ and AR LBDs, fluorescent micrographs of ligand-treated yeast cells were analyzed by densitometry using the program ImageJ [26] and expressed as the fold fluorescence change between ligand-treated and DMSO control cells (**Figure 5**).

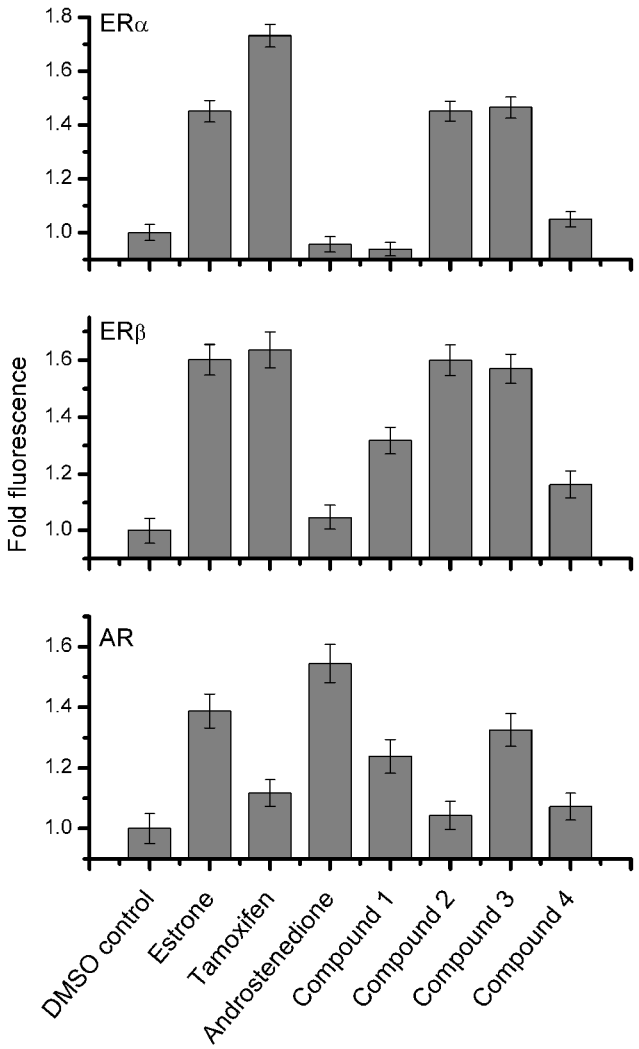

Figure 5. Fold fluorescence change between ligand-treated and DMSO control cells in the absence of ligand expressing ERα LBD-YFP, ERβ LBD-YFP and AR LBD-YFP measured by fluorescence microscopy. Fold fluorescence changes were calculated from fluorescence intensity per cell after 14-16 h exposure to 10 μM ligands or 1% DMSO, as a control. Higher values correspond to stronger binding affinity. Images were analyzed by densitometry using ImageJ freeware. Histograms were plotted using Origin Pro 8. Error bars represent propagated standard errors of the mean, based on analysis of 50 cells for each sample (n=50 cells)

Estrone and tamoxifen showed strong binding affinity for both ERα and ERβ, with fold fluorescence enhancements in the range of ~1.5 to 1.7 vs. controls, as expected. Similarly, androstenedione showed strong binding affinity for AR, with a fold fluorescence enhancement of ~1.5. Surprisingly, although tamoxifen had no affinity for AR as expected, estrone displayed

measureable affinity for the AR. This is in agreement with previous reports that estrone may be a weak agonist of AR signaling in transcription based yeast androgen assays [19].

Quantification of fluorescence microscopy results suggests that compounds **1-4** have much lower affinity for AR-LBD than . androstenedione (**Figure 5**). In contrast, compounds **2** and **3** appear to bind strongly to both ERα and ERβ isoforms by fluoresence microscopy, with affinitites comparable to estrone or tamoxifen. These results are in agreement with the reported antiestrogenic activities of **2** and **3** in uterotrophic assays [12,14].

3.3. Measurement of the relative binding affinities of ligands for ERα, ERβ and AR by fluorimetry in 96-well plates

To test if the assay can be used in high-throughput format, the same experiments were repeated using a 96-well fluoresence plate reader for measurements on intact yeast cells. Yeast expressing ERα LBD-YFP, ERβ LBD-YFP or AR-LBD-YFP were treated with test or control ligands and the fluoresence intensity of live yeast was measured in standard 96-well polystyrene plates. Ligand binding affinities for ERα, ERβ and AR were expressed as the fold fluorescence change between ligand-treated and DMSO control cells normalized for cell density and fluorescence values for uninduced cells. As can be seen from **Figure 6**, estrone and tamoxifen showed strong binding affinities for both ERα and ERβ, with 1.4-1.6 fold fluorescence enhancements compared to controls. Similarly, androstenedione showed binding affinity for AR, with a fold fluorescence enhancement of ~1.3. Negative controls estrone and tamoxifen had no measureable affinity for the AR, and androstenedione had no measureable affinity for either ER isoform.

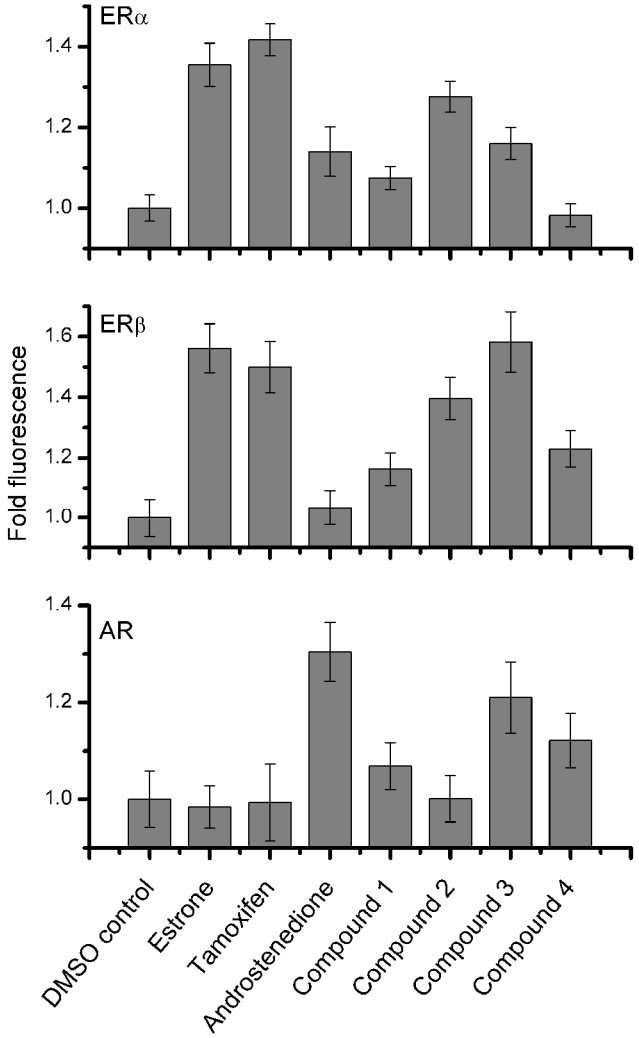

Figure 6. Fold fluorescence change between ligand-treated and DMSO control cells in the absence of ligand expressing ERα LBD-YFP, ERβ LBD-YFP and AR LBD-YFP measured by fluorimeter in 96-well format. Fold fluorescence change was calculated from fluorescence intensity per cell after 14-16 h exposure to 10 μM ligands and 1% DMSO, as a control. Histograms were plotted using Origin Pro 8. Error bars represent propagated standard errors of the mean.

Results from fluorescence spectroscopy also suggest that compounds **1-4** lack affinity for AR-LBD, in agreement with fluorescence microscopy analysis. Similarly, compound **2** was again found to have strong binding affinity for ERα and ERβ by fluorescence spectroscopy. In contrast, compound **3** appears to have strong affinity only for ERβ based on 96-well fluorescence spectroscopy measurements.

A comparison between fold fluorescence changes (ligand-treated vs. DMSO control cells) obtained by 96-well fluorescence spectroscopy and fluorescence microscopy is shown in **Figure 7**. As can be seen, there is qualitative agreement between these results, and both methods suggest that compounds **2** and **3** have affinity for ERα or ERβ.

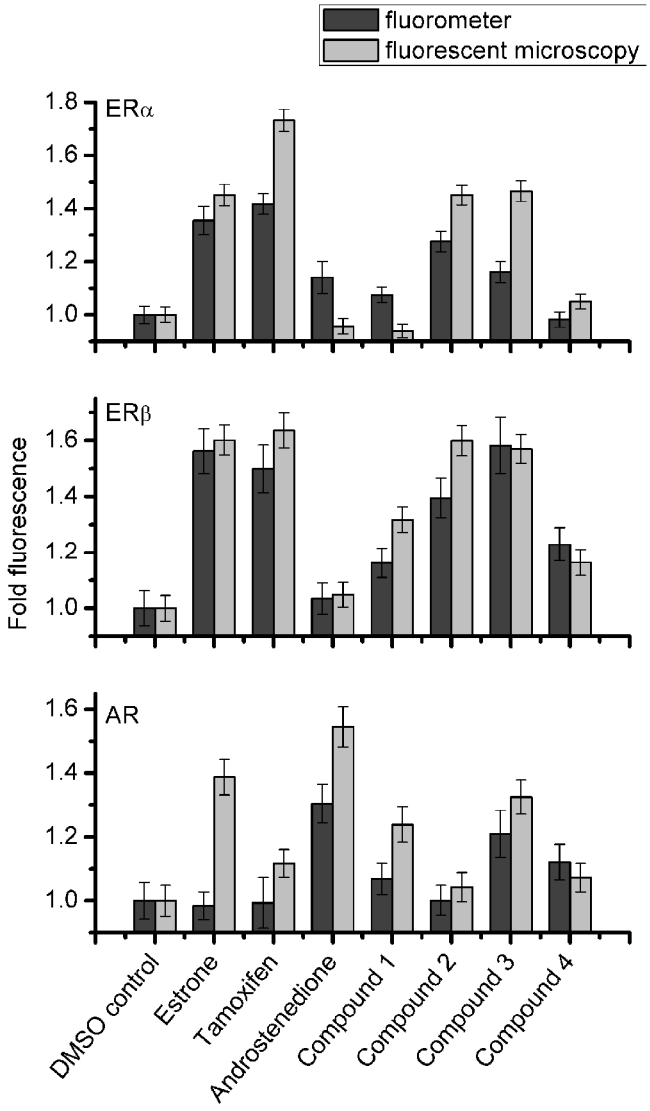

Figure 7. Comparison between fold fluorescence change between ligand-treated and DMSO control cells in the absence of ligand expressing ERα LBD-YFP, ERβ LBD-YFP and AR LBD-YFP measured by fluorimeter in 96-well format and fluorescence microscopy. Histograms were plotted using Origin Pro 8. Error bars represent propagated standard errors of the mean. Pearson's r correlation coefficients were also calculated to compare results obtained by the two methods: ERα LBD-YFP (r=0.87), ERβ LBD-YFP (r=0.94), AR LBD-YFP (0.95).

Based on these results, fluorescence measurements of intact yeast in 96-well format can be used as a rapid screen for identification of potential steroid receptor ligands, followed by further evaluation of the same cells using fluorescence microscopy. Fold fluorescence changes obtained by fluorescence microscopy were proportionally higher than those obtained by 96-well fluorescence spectroscopy, suggesting the higher sensitivity of individual cell analysis by fluorescence microscopy.

While the present assay is designed to measure the affinities of steroid derivatives for homodimeric steroid receptors, it is possible to develop a similar system to study heterodimeric steroid receptor pairs. This could be accomplished in yeast by either 1) fusing each steroid receptor LBD to a different 'FRET-compatible' fluorescent protein (*e.g.* YFP/CFP) [41] or 2) using a biomolecular fragment complementation (BiFC) approach involving split fluorescent proteins (e.g. split-YFP) [42]. Using our present assay, it would also be interesting to test the effects of co-expression of steroid receptor co-activators on ligand binding affinities [43].

3.4. *In vitro* antiproliferative activity of compounds 1-4

To further characterize the biological activities of tested compounds, we determined their antiproliferative potential against a panel of human cancer cell lines. Compounds **2**-**4** were tested for antiproliferative activity *in vitro* against two human cancer cell lines: MCF-7 and PC3 using the standard MTT assay [27]. Normal, non-cancerous MRC-5 cells were included as a control cell line and results were compared with the non-selective antiproliferative drug, doxorubicin. IC_{50} values for the antiproliferative activity of each compound are shown in **Table 1**.

Compound **1** has been reported previously to have submicromolar antiproliferative activity against both ER+ and ER- breast cancer cell lines, suggesting a mechanism of action

possibly involving molecular targets other than ER signaling [11]. Among tested compounds **2**-**4**, compound **2** displayed the strongest antiproliferative activity against the MCF-7 cell line, with an IC_{50} of 26.22 μM. MCF-7 breast adenocarcinoma cells express ER isoforms (ER+) and are considered to be estrogen senstive. This is in agreement with our results showing that compound **2** binds the LBD of ERα with high affinity. In addition, compound 2 was reported to have antiestrogenic activity [12]. Thus, it is possible that compound **2** may inhibit the growth of ER+ breast cancer cells by blocking the activity of ERα. While compound **3** was also found to have high affinity for ERα, it showed only low antiproliferative activity against MCF-7 cells. One possible explanation for this disparity is the fact that compound **3** is not as lipophillic as compound **2** (clogP=2.74 vs. 4.18) and may not cross the cell membrane as efficiently. Compound **4** displayed low antiproliferative activity against MCF-7 cells (IC_{50} 48.51 μM), in agreement with its negligible affinity for ERα. All test compounds showed low antiproliferative activity against PC3 cells, although the cytotoxicity of **4** was slightly greater with an IC_{50} 37.91 μM. Although PC3 cells express AR, their proliferation is considered to be hormone-independent [44]. Importantly, all tested steroid derivatives were non-toxic to normal MRC-5 cells, in contrast to doxorubicin which is highly cytotoxic. Doxorubicin controls showed low cytotoxicity against PC3 cells (IC_{50} 95.6 lM), in agreement with David-Beabes et al [45].

Table 1. Antiproliferative activity of compounds **2**-**4** and doxorubicin against two human cancer cell lines: MCF-7 and PC3 versus a normal non-cancerous control cell line, MRC-5. Antiproliferative activity

was determined using the MTT assay after exposure to 0.001, 0.01, 0.1, 1, 10 and 100 μM test compound for 48 h. Two independent experiments were conducted in quadruplicate for each concentration of test compound. Mean values and standard deviations were calculated for each concentration, and IC_{50} values were determined by Median effect analysis.

Compound	**IC50 (μM)**		
	MCF-7	**PC-3**	**MRC-5**[2]
2	26.22	63.42	>100
3	51.58	54.93	>100
4	48.51	37.91	>100
Doxorubicin[1]	0.75	95.61	0.12

[1]Control antiproliferative compound; [2]Non-cancerous control cells

3.4. Molecular docking of tested compounds against ERα and ERβ

Computational docking techniques, such as AutoDock, can correctly predict the geometry of ligands found in X-ray crystal structures, but have a lower accuracy of free energy prediction [46]. Thus, although docking programs can predict the corrrect geometry of protein-ligand interactions with very high accuracy, *ab initio* ranking of compounds based only on simulated docking energies may be problematic without experimental data [46]. However, in test libraries, sets of compounds that are predicted to bind tightly to a protein receptor are highly enriched with compounds that actually show binding by experimental measurements [46]. Therefore, in the present study we use molecular docking only to suggest possible binding geometries for compounds shown by fluorescence measurements to have high affinity for ERα or ERβ. Molecular docking simulations were conducted against the X-ray crystal structures of ERα-LBD (PDB ID: 1A52 [28]) and ERβ-LBD (PDB ID: 3OLS [29]) (**Table 2**). Control redocking simulations were conducted using estradiol, a natural steroidal ligand present in the X-ray crystal structures of both ER receptors, andreproduced accurate ligand-protein binding geometries present in the respective crystal structures (RMSD < 0.6 Å). Predicted binding energies ≤ -10.21

kcal/mol for ERα and ≤ -10.77 for ERβ were thus considered significant based on control redocking simulations.

Table 2. Comparison of experimental binding affinities of **1-4** for ERα and ERβ (fold fluoresence by microscopy) with molecular docking simulations (Autodock binding energies). Binding energies of ligands present in X-ray crystal structures were obtained from redocking simulations.

Compound	Fold fluorescence	Autodock binding energies (kcal/mol)
	ERα	
1	0.94	-10.31
2	1.45	-10.79
3	1.46	-10.37
4	1.05	n.b.[2]
Estrone	1.45	-10.15
Estradiol[1]	-	-10.21
	ERβ	
1	1.32	-10.55
2	1.60	-11.06
3	1.57	-10.79
4	1.16	n.b.[2]
Estrone	1.60	-10.66
Estradiol[1]	-	-10.77

[1]Ligand present in X-ray crystal structure (control); [2]Non-binding

Compound **1** was predicted by docking to have somewhat higher affinity for ERβ over ERα in agreement with our previous work [11]. However, docking studies predict a higher fold fluorescence change for **1** than observed in our experiments. Because **1** is strongly cytotoxic to ER- breast cancer cells that do not express ER, its mechanism of action likely involves other as yet unidentified protein target(s) [11].

In agreement with experimental measurements, molecular docking simulations suggest strong binding of compound **2** to ERα and ERβ isoforms, while compound **3** is predicted by docking to have stronger affinity for ERβ than ERα. As can be seen in **Figure 8**, compound **2** appears to be able to bind to both estrogen receptors in a similar orientation as estradiol, but with higher predicted binding affinity. Similar to X-ray structures of estradiol in complex with ER isoforms, the binding geometry of **2** also involves polar contacts between O3 and R394/346; and between H3 and E353/305 of ERα/ERβ [28,29]. However, the stronger predicted binding energy of compound **2** vs. estradiol could be due to halogen bonding between the 17-bromine modification and a conserved ER histidine residue (H524 for ERα and H475 of ERβ), which appears to mimic hydrogen bonding between the same histidine residue and O17 in estradiol. Depending on the context, halogen bonds can be stronger than hydrogen bonds [47].

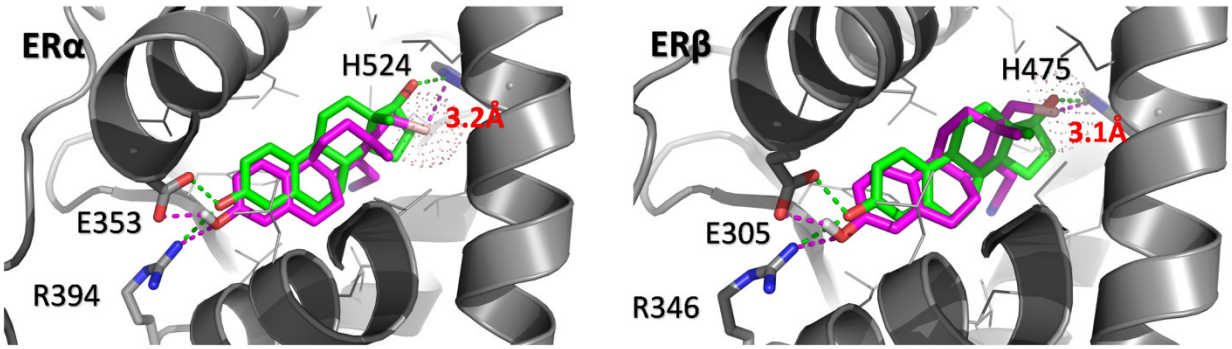

Figure 8. ERα (left) and ER β (right) docked with compound **2** (magenta), and estradiol (green). Compound **2** binds in similar orientation as estradiol and displays a similar network of hydrogen bonds, with the exception of a halogen bond formed between 17-bromine and H524 for ERα and H475 of ERβ.

The presence of a nitrile group on C16 of the steroid core also appears to correlate with binding affinity for ERs. Addition of a nitrile group modification has been shown to increase the binding of a synthetic ERβ ligand [48], and may contribute to the affinity of compound **2** for both ERs via hydrogen bonding. Compound **4** lacks a nitrile moiety, which we speculate might

be a possible cause for its lower affinity for ERα and ERβ. Results from molecular docking could be combined with fluorescence and other data to help design steroidal derivatives with higher affinity and selectivity for ERα or ERβ that could be tested in the assay described here.

4. Conclusions

The relative binding affinities of D-seco modified steroid derivatives **1-4** were estimated for the ligand binding domains of estrogen receptor α, estrogen receptor β or androgen receptor using an optimized non-transcriptional fluorescent cell assay in yeast. Based on these results a D-seco estratriene derivative **2** with a 17-bromine modification displays selective estrogen receptor binding and *in vitro* cytotoxicity against MCF-7 estrogen receptor positive breast adenocarcinoma cells. The assay described here can identify potential modulators of steroid receptor signaling or help filter out compounds with off-target affinity for steroid receptors.

Acknowledgements

This work was supported by the Ministry of Education, Science and Technological Development of the Republic of Serbia [grant number 172021].

5. References

[1] N. Ahmad, R. Kumar, Steroid hormone receptors in cancer development: a target for cancer therapeutics, Cancer Lett. 300 (2011) 1–9. doi:10.1016/j.canlet.2010.09.008.

[2] A.C. Herington, L.K. Chopin, P. Jeffery, L. De Amorim, T. Veveris-Lowe, L. Bui, J.A. Clements, Hormone-dependent cancers: new approaches to identification of potential diagnostic and/or therapeutic biomarkers, Asia Pac. J. Mol. Biol. Biotechnol. (2010) 63–66.

[3] R. Kumar, B.H. Johnson, E.B. Thompson, Overview of the structural basis for transcription regulation by nuclear hormone receptors, Essays Biochem. 40 (2004) 26–39. doi:10.1042/bse0400027.

[4] N. Heldring, A. Pike, S. Andersson, J. Matthews, G. Cheng, J. Hartman, M. Tujague, A. Ström, E. Treuter, M. Warner, J.Å. Gustafsson, Estrogen receptors: how do they signal and what are their targets, Physiol. Rev. 87 (2007) 905–931. doi:10.1152/physrev.00026.2006.

[5] Y. Omoto, H. Iwase, Clinical significance of estrogen receptor β in breast and prostate cancer from biological aspects, Cancer Sci. 106 (2015) 337–343. doi:10.1111/cas.12613.

[6] F. Castiglione, A. Taddei, D.R. Degl'Innocenti, A.M. Buccoliero, P. Bechi, F. Garbini, F.G. Chiara, D. Moncini, G. Cavallina, L. Marascio, G. Freschi, L.T. Gian, Expression of estrogen receptor beta in colon cancer progression, Diagn. Mol. Pathol. 17 (2008) 231–236. doi:10.1097/PDM.0b013e3181656d67.

[7] C.A. Heinlein, C. Chang, Androgen receptor in prostate cancer, Endocr. Rev. 25 (2004) 276–308. doi:10.1210/er.2002-0032.

[8] C.I. Lee, A. Goodwin, N. Wilcken, Fulvestrant for hormone-sensitive metastatic breast cancer, Cochrane Database Syst. Rev. (2017) CD011093. doi:10.1002/14651858.CD011093.pub2.

[9] L. Gennari, D. Merlotti, R. Nuti, Selective estrogen receptor modulator (SERM) for the treatment of osteoporosis in postmenopausal women: focus on lasofoxifene, Clin. Interv. Aging. 5 (2010) 19–29. doi:10.2147/CIA.S6083.

[10] J. V. Pinkerton, S. Thomas, Use of SERMs for treatment in postmenopausal women, J. Steroid Biochem. Mol. Biol. 142 (2014) 142–154. doi:10.1016/j.jsbmb.2013.12.011.

[11] A.R. Nikolić, E.T. Petri, O.R. Klisurić, A.S. Ćelić, D.S. Jakimov, E.A. Djurendić, K.M. Penov Gaši, M.N. Sakač, Synthesis and anticancer cell potential of steroidal 16,17-seco-16,17a-dinitriles: identification of a selective inhibitor of hormone-independent breast cancer cells, Bioorg. Med. Chem. 23 (2015) 703–711. doi:10.1016/j.bmc.2014.12.069.

[12] S. Jovanović-Šanta, J. Petrović, S. Andrić, R. Kovačević, E. Djurendić, M. Sakač, D. Lazar, S. Stanković, Synthesis, structure, and screening of estrogenic and antiestrogenic activity of new 3,17-substituted-16,17-seco-estratriene derivatives, Bioorg. Chem. 31 (2003) 475–484. doi:10.1016/S0045-2068(03)00101-9.

[13] S.S. Jovanović-Šanta, V.M. Pejanović, J.A. Petrović, A novel route to 3-hydroxy-16 , 17-seco-estrone derivatives, J. Serb. Chem. Soc. 64 (1999) 391–394.

[14] M.N. Sakač, D.A. Miljković, K.M. Penov Gaši, M. Popsavin, O.R. Klisurić, S.M. Stanković, S. Andrić, R. Kovačević, Synthesis, X-ray crystal structure and antiestrogenic activity of 17-methyl-16,17-secoestra-1,3,5(10)-triene derivatives, Collect. Czechoslov. Chem. Commun. 70 (2005) 63–71. doi:10.1135/cccc20050063.

[15] J.A. Petrović, V.M. Pejanović, D.A. Miljković, J.T. Hranisavljević, Synthesis and

estrogen activity screening of some new D-secoestrone derivatives, Steroids. 55 (1990) 276–278. doi:10.1016/0039-128X(90)90045-D.
[16] B.E. Herman, J. Szabó, I. Bacsa, J. Wölfling, G. Schneider, M. Bálint, C. Hetényi, E. Mernyák, M. Szécsi, Comparative investigation of the in vitro inhibitory potencies of 13-epimeric estrones and D-secoestrones towards 17 β -hydroxysteroid dehydrogenase type 1, J. Enzym. Inhib. Med. Chem. 31 (2016) 61–69. doi:10.1080/14756366.2016.1204610.
[17] T.F.H. Bovee, R.J.R. Helsdingen, A.R.M. Hamers, R.J.R. van Duursen, M.W.F. Nielen, R.L.A.P. Hoogenboom, A new highly specific and robust yeast androgen bioassay for the detection of agonists and antagonists, Anal. Bioanal. Chem. 389 (2007) 1549–1558. doi:10.1007/s00216-007-1559-6.
[18] F. Köhler, A. Zimmermann, M. Hager, A.E. Sippel, A genetic, non-transcriptional assay for nuclear receptor ligand binding in yeast binding in yeast, Gene. 337 (2017) 113–119. doi:10.1016/j.gene.2004.04.018.
[19] ICCVAM Evaluation of In Vitro Methods for Detecting Potential ED.pdf, (2003). available: https://ntp.niehs.nih.gov/ (accessed 05. 06. 2017).
[20] S.S. Muddana, B.R. Peterson, Fluorescent cellular sensors of steroid receptor ligands, ChemBioChem. 4 (2003) 848–855. doi:10.1002/cbic.200300606.
[21] X. Shi, J. Basran, H.E. Seward, W. Childs, C.R. Bagshaw, S.G. Boxer, Anomalous negative fluorescence anisotropy in Yellow Fluorescent Protein (YFP 10C): Quantitative analysis of FRET in YFP dimers, Biochemistry. 46 (2007) 14403–14417. doi:10.1021/bi701575n.
[22] D. Gietz, A. St Jean, R.A. Woods, R.H. Schiestl, Improved method for high efficiency transformation of intact yeast cells, Nucleic Acid Res. 20 (1992) 1425. doi:10.1093/nar/20.6.1425.
[23] R.K. Mann, M. Grunstein, Histone H3 N-terminal mutations allow hyperactivation of the yeast GAL1 gene in vivo, EMBO J. 11 (1992) 3297–3306.
[24] T. Barkhem, B. Carlsson, Y. Nilsson, E. Enmark, J.-Å. Gustafsson, S. Nilsson, Differential response of estrogen receptor alpha and estrogen receptor beta to partial estrogen agonists/antagonists, Mol. Pharmacol. 54 (1998) 105–112. doi:10.1124/mol.54.1.105.
[25] R.Y. Tsien, The green fluorescent protein, Annu. Rev. Biochem. 67 (1998) 509–544. doi:10.1146/annurev.biochem.67.1.509.
[26] J. Schindelin, I. Arganda-Carreras, E. Frise, V. Kaynig, M. Longair, T. Pietzsch, S. Preibisch, C. Rueden, S. Saalfeld, B. Schmid, J.-Y. Tinevez, D.J. White, V. Hartenstein, K. Eliceiri, P. Tomancak, A. Cardona, Fiji: an open source platform for biological image analysis, Nat. Methods. 9 (2012) 676–682. doi:10.1038/nmeth.2019.
[27] T. Mosmann, Rapid colorimetric assay for cellular growth and survival: application to proliferation and cytotoxicity assay, J. Immunol. Methods. 65 (1983) 55–63. doi:10.1016/0022-1759(83)90303-4.
[28] D.M. Tanenbaum, Y. Wang, S.P. Williams, P.B. Sigler, Crystallographic comparison of the estrogen and progesterone receptor's ligand binding domains, Proc. Natl. Acad. Sci. U.S.A. 95 (1998) 5998–6003. doi:10.1073/pnas.95.11.5998.
[29] S. Möcklinghoff, R. Rose, M. Carraz, A. Visser, C. Ottmann, L. Brunsveld, Synthesis and crystal structure of a phosphorylated estrogen receptor ligand binding domain, ChemBioChem. 11 (2010) 2251–2254. doi:10.1002/cbic.201000532.
[30] RCSB Protein Data Bank (PDB), (2017). http://www.rcsb.org/ (accessed March 30, 2017).

[31] H.M. Berman, J. Westbrook, Z. Feng, G. Gilliland, T.N. Bhat, H. Weissig, I.N. Shindyalov, P.E. Bourne, The protein data bank, Nucleic Acids Res. 28 (2000) 235–242. doi:10.1093/nar/28.1.235.
[32] A. Pedretti, L. Villa, G. Vistoli, Atom-type description language: a universal language to recognize atom types implemented in the VEGA program, Theor. Chem. Acc. 109 (2003) 229–232. doi:10.1007/s00214-002-0402-6.
[33] Avogadro: an open-source molecular builder and visualization tool. Version 1.1.1., (2017). https://avogadro.cc/ (accessed March 30, 2017).
[34] M.D. Hanwell, D.E. Curtis, D.C. Lonie, T. Vandermeersch, E. Zurek, G.R. Hutchison, Avogadro: an advanced semantic chemical editor, visualisation, and analysis platform, J. Chem. Informatics. 4 (2012) 1–17. doi:10.1016/S0968-0004(00)89080-5.
[35] G.M. Morris, R. Huey, W. Lindstrom, M.F. Sanner, R.K. Belew, D.S. Goodsell, A.J. Olson, AutoDock4 and AutoDockTools4: automated docking with selective receptor flexibility, J. Comput. Chem. 30 (2009) 2785–2791. doi:10.1002/jcc.21256.
[36] The PyMOL Molecular Graphics System, Version 1.8 Schrödinger, LLC., (2017). https://www.pymol.org (accessed March 30, 2017).
[37] J. Ren, N. Williams, L. Clementi, S. Krishnan, W.W. Li, Opal web services for biomedical applications, Nucleic Acids Res. 38 (2010) 724–731. doi:10.1093/nar/gkq503.
[38] NBCR-National Biomedical Computation Resource, (2017). http://nbcr-222.ucsd.edu/opal2/services (accessed March 30, 2017).
[39] L.K. Wolf, New software and websites for the chemical enterprise, Chem. Eng. News. 87 (2009) 48. doi:10.1021/cen-v087n045.p048.
[40] A. Brodie, V. Njar, L.F. Macedo, V.T. Sean, G. Sabnis, Steroidogenic enzyme inhibitors and hormone dependent cancer, Urol. Oncol. 27 (2009) 53–63. doi:10.1016/j.urolonc.2008.07.036.
[41] S. De, I.G. Macara, D.A. Lannigan, Novel biosensors for the detection of estrogen receptor ligands, J. Steroid Biochem. Mol. Biol. 96 (2005) 235–244. doi:10.1016/j.jsbmb.2005.04.030.
[42] E. Barnard, N.V. McFerran, A. Trudgett, J. Nelson, D.J. Timson, Development and implementation of split-GFP-based bimolecular fluorescence complementation (BiFC) assays in yeast, Biochem. Soc. Trans. 36 (2008) 479–482. doi:10.1042/BST0360479.
[43] D.L. Stenoien, A.C. Nye, M.G. Mancini, K. Patel, M. Dutertre, B.W. O'Malley, C.L. Smith, A.S. Belmont, M.A. Mancini, Ligand-mediated assembly and real-time cellular dynamics of estrogen receptor alpha-coactivator complexes in living cells, Mol. Cell. Biol. 21 (2001) 4404–4412. doi:10.1128/MCB.21.13.4404-4412.2001.
[44] S. Tai, Y. Sun, J.M. Squires, W.K. Oh, H. Zhang, C.-Z. Liang, J. Huang, PC3 is a cell line characteristic of prostatic small cell carcinoma, Prostate. 71 (2012) 1668–1679. doi:10.1002/pros.21383.PC3.
[45] G.L. David-Beabes, M.J. Overman, J.A. Petrofski, P.A. Campbell, A.M.D.E. De Marzo, W.G. Nelson, Doxorubicin-resistant variants of human prostate cancer cell lines DU 145 , PC-3, PPC-1, and TSU-PR1 : characterization of biochemical determinants of antineoplastic drug sensitivity, Inter. J. Oncol. 177 (2000) 1077–1086.
[46] S. Cosconati, S. Forli, A.L. Perryman, R. Harris, S. David, A.J. Olson, Virtual Screening with AutoDock: theory and practice, Expert Opin. Discov. 5 (2011) 597–607. doi:10.1517/17460441.2010.484460.
[47] L.P. Wolters, F.M. Bickelhaupt, Halogen bonding versus hydrogen bonding: a molecular

orbital perspective, ChemistryOpen. 1 (2012) 96–105. doi:10.1002/open.201100015.
[48] E.S. Manas, R.J. Unwalla, Z.B. Xu, M.S. Malamas, C.P. Miller, H.A. Harris, C. Hsiao, T. Akopian, W.T. Hum, K. Malakian, S. Wolfrom, A. Bapat, R.A. Bhat, M.L. Stahl, W.S. Somers, J.C. Alvarez, Structure-based design of estrogen receptor-beta selective ligands, J. Am. Chem. Soc. 126 (2004) 15106–15119. doi:10.1021/ja047633o.

Highlights

- Relative binding affinities of D-seco modified steroid derivatives were estimated for estrogen receptor α, estrogen receptor β or androgen receptor using an optimized non-transcriptional fluorescent cell assay in yeast.
- D-seco estratriene derivative **2** displays selective estrogen receptor binding and *in vitro* cytotoxicity against MCF-7 estrogen receptor positive breast adenocarcinoma cells.
- The assay described here can identify potential modulators of steroid receptor signaling or filter out compounds with off-target affinity for steroid receptors.